The Role of Meteorological Conditions and Pollution Control Strategies in Reducing Air Pollution in Beijing during APEC 2014 and Parade 2015

Pengfei Liang[1], Tong Zhu[1*], Yanhua Fang[1], Yingruo Li[1, 2], Yiqun Han[1], Yusheng Wu[1], Min Hu[1], and Junxia Wang[1]

[1]SKL-ESPC and BIC-ESAT, College of Environmental Sciences and Engineering, Peking University, Beijing, 100871, China

[2]Environmental Meteorology Forecast Center of Beijing-Tianjin-Hebei, China Meteorological Administration, Beijing, 100089, China

[*]Correspondence to: Tong Zhu (tzhu@pku.edu.cn)

Abstract

To control severe air pollution in China, comprehensive pollution control strategies have been implemented throughout the country in recent years. To evaluate the effectiveness of these strategies, the influence of meteorological conditions on levels of air pollution needs to be determined. Using the intensive air pollution control strategies implemented during the Asia-Pacific Economic Cooperation Forum in 2014 (APEC 2014) and the Victory Parade for the Commemoration of the 70th Anniversary of the Chinese Anti-Japanese War and the World Anti-Fascist War in 2015 (Parade 2015) as examples, we estimated the role of meteorological conditions and pollution control

strategies in reducing air pollution levels in Beijing. Atmospheric particulate matter of aerodynamic diameter ≤ 2.5 μm ($PM_{2.5}$) samples were collected and gaseous pollutants (SO_2, NO, NO_x, and O_3) were measured online at a site in Peking University (PKU). To determine the influence of meteorological conditions on the levels of air pollution, we first compared the air pollutant concentrations during days with stable meteorological conditions. However, there were few days with stable meteorological conditions during Parade. As such, we were unable to estimate the level of emission reduction efforts during this period. Finally, a generalized linear regression model (GLM) based only on meteorological parameters was built to predict air pollutant concentrations, which could explain more than 70% of the variation in air pollutant concentration levels, after incorporating the nonlinear relationships between certain meteorological parameters and the concentrations of air pollutants. Evaluation of the GLM performance revealed that the GLM, even based only on meteorological parameters, could be satisfactory to estimate the contribution of meteorological conditions in reducing air pollution, and hence the contribution of control strategies in reducing air pollution. Using the GLM, we found that the meteorological conditions and pollution control strategies contributed 30% and 28% to the reduction of the $PM_{2.5}$ concentration during APEC, and 38% and 25% during Parade, based on the assumption that the concentrations of air pollutants are only determined by meteorological conditions and emission intensities. We also estimated the contribution of meteorological conditions and control strategies in reducing the concentrations of gaseous pollutants and $PM_{2.5}$ components with the GLMs, revealing the effective control of anthropogenic emissions.

1 Introduction

Air pollution poses serious health risks to human populations and is one of the most important global environmental problems. To control air pollution in China, the State Council of China (2013) has released the Action Plan for Air Pollution Prevention and Control, which sets pollution control targets for different regions, e.g. atmospheric particulate matter of aerodynamic diameter ≤ 2.5 μm ($PM_{2.5}$) concentrations in 2017 shall fall in Beijing–Tianjin–Hebei (BTH) by 25%, in the Yangtze River Delta by 20%, and in the Pearl River Delta by 15%, compared with the levels of 2012. To meet these targets, comprehensive pollution control strategies have been implemented at the national, provincial, and city levels. However, it is not clear how effective these strategies are in reducing air pollution. One of the challenges in evaluating the effectiveness of these strategies is that the long-term strategies cannot improve air quality in the short term. The efforts made to ensure satisfactory air quality for special events in the short term, such as the Beijing 2008 Olympics, provide a unique opportunity to evaluate the effectiveness of pollution control strategies (Kelly and Zhu, 2016). During the Beijing Olympics comprehensive pollution control strategies were implemented intensively over a short period of time. Based on the successful experience during this event, the Chinese government implemented similar air pollution control measures for the 41st Shanghai World Expo in 2010 (Huang et al., 2012; SEPB, 2010), the 16th Guangzhou Asian Games and Asian Para Games in 2010 (GEPB, 2009; Liu et al., 2013), and the Chengdu Fortune Forum 2013 (CEPB, 2013). To ensure satisfactory air quality in Beijing during the two most recent events: APEC 2014 and Parade 2015,

65 the Chinese central government and the local government in Beijing, together with its
66 surrounding provinces, implemented comprehensive air pollution control strategies.
67 These two events provide a good opportunity to evaluate the effectiveness of air
68 pollution control strategies.

69 One challenge when evaluating the effectiveness of air pollution control strategies
70 over a short period of time is separating out the contribution of meteorological
71 conditions to the reduction in air pollution levels.

72 Most previous studies have only provided a descriptive analysis of the changing
73 concentrations of air pollutants during these events. Wen et al. (2016) reported that the
74 average $PM_{2.5}$ concentration during APEC decreased by 54%, 26%, and 39% compared
75 with the levels before APEC in Beijing, Shijiazhuang, and Tangshan, respectively. Han
76 et al. (2015) observed that the extinction coefficient and absorbance coefficient
77 decreased significantly during APEC compared with the values before APEC.

78 An increasing number of studies have recognized the importance of
79 meteorological conditions in determining air pollution in Beijing and North China Plain
80 (Calkins et al., 2016; Zhang et al., 2012). A northerly wind is considered to be
81 favourable for pollutant diffusion, while a southerly wind is considered to be favourable
82 for the transport of pollutants to Beijing (Zhang et al., 2014). When assessing the
83 effectiveness of air pollution control strategies, a few studies have distinguished
84 between the contribution of meteorological conditions and pollution control strategies
85 in reducing air pollution by comparing air pollutant concentrations under similar
86 meteorological conditions (Wang et al., 2015; Zhang et al., 2009). However, in these

studies, days with stable meteorological conditions were determined subjectively, which may introduce uncertainties and inconsistencies when estimating changes in air pollutant concentrations.

Statistical models have been developed to establish the relationship between air pollutant concentrations and meteorological parameters. Table 1 summarizes these models, with their respective R^2 values. Multiple linear regression models have been widely applied to demonstrate the quantitative relationship between air pollutant concentrations and meteorological parameters, by assuming a linear relationship. However, these relationships are often non-linear (Liu et al., 2007; Liu et al., 2012). Most of the models with good explanation ($R^2 > 0.6$) have actually adopted visibility, aerosol optical depth (AOD), and air quality index (AQI) as independent variables to improve the performance of the regression models (Liu et al., 2007; Sotoudeheian and Arhami, 2014; Tian and Chen, 2010; You et al., 2015). This could cause problems in the prediction of air pollutant concentrations during intensive emission control periods because visibility, AOD, and AQI are also dependent on air pollution levels; hence, the statistical models may not function when air pollutant levels are drastically reduced over a short period. A statistical model based solely on meteorological parameters to predict air pollutant concentrations is therefore required.

In this study, we used the air pollution control periods during APEC 2014 and Parade 2015 to estimate the role of meteorological conditions and pollution control strategies in reducing air pollution in the megacity of Beijing. We first measured the changes in air pollutant concentrations, including $PM_{2.5}$, gaseous pollutants, and the

components of $PM_{2.5}$. We then estimated the role of meteorological conditions and pollution control strategies in reducing air pollution by comparing the pollutant concentrations during days with stable meteorological conditions. Finally, we developed a statistical model based only on meteorological parameters to evaluate the role of meteorological conditions and pollution control strategies in reducing the levels of air pollution in Beijing.

2 Measurements and Methods

2.1 Measurements

2.1.1 Measurements of Air Pollutants

Gaseous pollutants (SO_2, NO, NO_x, and O_3) were measured online, and $PM_{2.5}$ samples were collected on filters at an urban monitoring station in the campus of Peking University (39.99°N, 116.33°E) northwest of Beijing (Huang et al., 2010). The station is located on the roof of a six-floor building, about 20 m above the ground and about 550 m north of the 4^{th} Ring Road of Beijing.

A $PM_{2.5}$ four-channel sampler (TH-16A, Wuhan Tianhong Instruments Co., Ltd., Hubei, China) was used to collect $PM_{2.5}$ samples. The sampling duration was 23.5 h (from 09:30 to 09:00 LT the next day). Both 47-mm quartz filters (QM/A, Whatman, Maidstone, England) and Teflon filters (PTFE, Whatman) were used. The flow rate was calibrated to 16.7 L min^{-1} each week and a blank $PM_{2.5}$ sample was collected once a month. The quartz filters were baked at 550°C for 5.5 h before use. Immediately after collection, the filter samples were stored at −25°C until analysis.

Sulphur dioxide (SO_2) was measured with an SO_2 analyzer (43i TL, Thermo Fisher Scientific, Waltham, MA, USA), with a precision of 0.05 ppb. Nitric oxide (NO) and nitrogen oxides (NO_x) were measured with a NO-NO_x analyzer (42i TL, Thermo Fisher Scientific), with precisions of 0.05 ppb for NO and 0.17 ppb for NO_2. Ozone (O_3) was measured with an O_3 analyzer (49i, Thermo Fisher Scientific), with a precision of 1.0 ppb. The SO_2 and NO-NO_x analyzers both had a detection limit of 0.05 ppb, and the O_3 analyzer had a detection limit of 0.50 ppb. All of the gaseous pollutant analyzers had a time resolution of 1 min, and were maintained and calibrated weekly following the manufacturer's protocols.

2.1.2 Meteorological Data

Meteorological data were obtained from the National Climate Data Center (www.ncdc.noaa.gov) dataset. The meteorological parameters were monitored at a station located in the Beijing Capital International Airport, and consisted of temperature (T), relative humidity (RH), wind direction (WD), wind speed (WS), sea level pressure (SLP), and precipitation (PREC). The PBL height was computed from the simulation results of the National Center for Environmental Prediction (NCEP) Global Data Assimilation System (GDAS) model (www.ready.arl.noaa.gov/READYamet.php).

2.1.3 Analysis of the $PM_{2.5}$ Filter Samples

To obtain daily average $PM_{2.5}$ mass concentrations, Teflon filters were weighed before and after sampling using an electronic balance, with a detection limit of 10 μg (AX105DR) in a super-clean lab (T: 20 ± 1°C, RH: 40 ± 3%). A portion of each Teflon

filter was extracted with ultrapure water for the measurement of water-soluble ions (Na^+, NH_4^+, K^+, Mg^{2+}, Ca^{2+}, SO_4^{2-}, NO_3^-, and Cl^-), with an ion-chromatograph (IC-2000 & 2500, Dionex, Sunnyvale, CA, USA). The detection limits of Na^+, NH_4^+, K^+, Mg^{2+}, Ca^{2+}, SO_4^{2-}, NO_3^-, and Cl^- were 0.03, 0.06, 0.10, 0.10, 0.05, 0.01, 0.01, and 0.03 mg L^{-1}, respectively. A portion of each Teflon filter was digested with a solution consisting of nitric acid (HNO_3), hydrochloric acid (HCl), and hydrofluoric acid (HF) for the measurement of trace elements (Na, Mg, Al, Ca, Mn, Fe, Co, Cu, Zn, Se, Mo, Cd, Ba, Tl, Pb, Th and U), with inductively coupled plasma-mass spectrometry (ICP-MS, Thermo X series, Thermo Fisher Scientific). The recoveries for all measured elements fell within ±20% of the certified values. A semi-continuous organic carbon/elemental carbon (OC/EC) analyzer (Model 4, Sunset Laboratory, Tigard, OR, USA) was used to analyze organic and elemental carbon from a round punch (diameter: 17 mm) from each quartz filter sample. The T protocol of the National Institute for Occupational Safety and Health (NIOSH) thermal-optical method was applied (see details in Table S1).

All analytical instruments were calibrated before each series of measurements. The R^2 values of the calibration curves for ions, elements, and sucrose concentrations were higher than 0.999.

2.2 Research Periods Definition and Control Strategies

In our study, the APEC 2014 campaign consisted of three distinct periods: before APEC (18 October to 2 November 2014), during APEC (3 to 12 November 2014), and after APEC (13 to 22 November 2014). The Parade 2015 campaign was also divided

into three distinct periods: before Parade (1 to 19 August 2015), during Parade (20 August to 3 September 2015), and after Parade (4 to 23 September 2015). A total of 225 $PM_{2.5}$ filter samples were collected from 1 October to 31 December 2014 and from 1 August to 31 December 2015. Sufficient number of sampling days are used to establish the relationship between air pollutant concentrations and meteorological parameters. 20 days of $PM_{2.5}$ samples were missed due to rain or sampler failures.

Table 2 shows the control periods and control strategies of APEC and Parade. , including the control of emissions from traffic, industry, and coal combustion, as well as dust pollution.

2.3 Methods for the Meteorological Conditions Separation

2.3.1 Identify Stable Meteorological Periods

Stable conditions can be defined based on the relationship between air pollution levels and both WSs and PBL height. Figure 5 shows scatter plots between $PM_{2.5}$ concentrations and WS and PBL heights. The relationship can be fitted with a power function. A stable condition could be defined by identifying the turning points when the slopes changed from large to relatively small values, and stable conditions could be defined when WSs and PBL heights were lower than the values of the turning points.

The slopes of the power function were monotone, varying with no inflection point. Thus, we used piecewise functions to identify the turning points. As Figure 5 shows, the intersections of two fitting lines represented the turning points of the meteorological influence on $PM_{2.5}$; thus, we defined days with stable meteorological conditions to be

193 those with a daily average WS less than 2.50 m s^{-1} and a daily average PBL height
194 lower than 290 m. We could then compare the corresponding pollutant concentrations
195 between days with stable meteorological conditions.

196 Figure 5 here

197 **2.3.2 Generalized Linear Regression Model (GLM)**

198 A GLM was used to establish the relationship between air pollutant concentrations
199 and meteorological parameters. The objective dependent variables included
200 concentrations of $PM_{2.5}$, individual $PM_{2.5}$ components, and gaseous pollutants.

201 To match the 23.5-h (09:30–09:00 LT the next day) sampling time of the $PM_{2.5}$
202 filter samples, metrological parameters were averaged over the same time span (Table
203 3) and used in the GLM alongside other parameters, e.g. the daily maximum of certain
204 meteorological parameters. The meteorological parameters used in the GLM were T,
205 RH, WD, WS, PBL height, SLP, and PREC. WDs were grouped into three categories,
206 with relevant values and assigned to each category: north (NW, W and NE) as 1, south
207 (SW, SE and E) as 2, and "calm and variable" as 3. A calm wind was defined as when
208 the WS was less than 0.5 m s^{-1}. According to the JetStream Glossary of NOAA
209 (http://www.srh.weather.gov/srh/jetstream/append/glossary_v.html), a variable WD
210 was defined as a condition when: (1) the WD fluctuated by 60° or more during a 2-min
211 evaluation period, with a WS greater than 6 knots (11 km h^{-1}); or (2) the WD was
212 variable and the WS was less than 6 knots (11 km h^{-1}).

213 A preliminary analysis showed that the concentrations of air pollutants and

meteorological parameters fitted best with an exponential function or power function (Figure S2); therefore, these functions were natural log transformed and introduced into the GLM.

We applied the stepwise method to evaluate the level of multicollinearity between the independent variables based on relevant judgement indexes, such as the variance inflation factor (VIF) or tolerance. Based on the assumption that the regression residuals followed a normal distribution and homoscedasticity, which is discussed in a later section, we developed the following model to calculate the concentrations of air pollutants and chemical components of $PM_{2.5}$ based on meteorological parameters:

$$ln\,C_{ij} = \beta_0 + \sum_{k=1}^{m} \beta_{1k} x_k + \sum_{k=1}^{n} \beta_{2k} ln\,x_k + \sum_{k=1}^{m'} \beta_{3k} x_k\,(lag) + \sum_{k=1}^{n'} \beta_{4k} ln\,x_k\,(lag) \quad (1)$$

where C_{ij} is the concentration of the j^{th} air pollutant averaged over the i^{th} day, x_k is the k^{th} meteorological parameter, β_k is the regression coefficient of the k^{th} meteorological parameter, and β_0 is the intercept. For meteorological parameters containing both positive and negative values (i.e. T), only the exponential form was applied. *m*, *n*, *m'*, and *n'* are the number of different forms of meteorological parameters that were eventually included in the model, and were determined based on the stepwise entering method of the regression model. The suffix of *(lag)* refers to the meteorological parameters of the previous day. The main assumption for equation (1) was that the concentrations of air pollutants were only a function of the meteorological parameters, and the emission intensities were constant. Hence, we only used the data before and after APEC 2014 and Parade 2015 control periods in equation (1), excluding the data collected during each period and during the heating season, e.g. after 15 November

2014.

Compared with the models used in previous studies (Table 1), our statistical model had the following advantages: (1) all of the independent variables were meteorological parameters; (2) we considered the non-linear relationships between air pollutant concentrations and meteorological parameters; and (3) in addition to predicting $PM_{2.5}$ mass concentrations, our model could also predict concentrations of gaseous pollutants and individual $PM_{2.5}$ components by corresponding models for different pollutants.

3 Results and Discussion

3.1 Changes of Air Pollutant Concentrations during the APEC 2014 and Parade 2015 Campaigns

Figure 1 shows the time series of $PM_{2.5}$ and the concentrations of its components, as well as the meteorological parameters during the APEC 2014 and Parade 2015 campaigns.

There were two pollution episodes during APEC, on 4 November and 7–10 November 2014, which corresponded to two relatively stable periods with low WS, mainly from the south. The T declined gradually from 12.2°C before APEC to 4.9°C after APEC, and the RH was above 60% during the two pollution episodes. During Parade, the $PM_{2.5}$ concentrations were low, with the prevailing WD from the north and low WS. The T was mostly higher than 20°C, which differed from that during the APEC campaign when it was lower than 20°C.

Table 4 lists the mean concentrations and standard deviations of $PM_{2.5}$, gaseous

pollutants, and $PM_{2.5}$ components during the APEC and Parade campaigns. The mean concentration of $PM_{2.5}$ during APEC was 48 ± 35 μg m^{-3}, 58% lower than before APEC (113 ± 62 μg m^{-3}), and 51% lower than after APEC (97 ± 84 μg m^{-3}). The mean concentration of $PM_{2.5}$ during Parade was 15 ± 6 μg m^{-3}, 63% lower than before Parade (41 ± 14 μg m^{-3}), and 62% lower than after Parade (39 ± 28 μg m^{-3}).

Figure 1 here

Figure 2 shows the proportion of the measured $PM_{2.5}$ components, including OC; EC; the sum of the sulphate, nitrate, and ammonia (SNA); and chloride ion (Cl^-) and trace elements, which together accounted for 70–80% of the total $PM_{2.5}$ mass concentration. The proportions of OC (23.5%) and EC (3.5%) in $PM_{2.5}$ were highest during APEC. The proportion of SNA in $PM_{2.5}$ during APEC (40.6%) was lower than before APEC (50.7%) and higher than after APEC (37.2%). The proportions of Cl^- (4.3%) and elements (6.8%) in $PM_{2.5}$ during APEC were higher than before APEC and lower than after APEC. For the Parade campaign, the proportions of OC (26.6%) and elements (6.6%) in $PM_{2.5}$ were highest during Parade. The proportions of EC (4.9%) and Cl^- (1.1%) in $PM_{2.5}$ during Parade were higher than before Parade and lower than after Parade. The proportion of SNA in $PM_{2.5}$ was lowest during Parade (37.3%). Similarly, during the pollution control periods of APEC and Parade, the proportions of OC and elements in $PM_{2.5}$ tended to increase and the proportion of SNA in $PM_{2.5}$ tended to decrease.

Figure 2 here

EC is usually considered to be a marker of anthropogenic primary sources, while the

sources of OC include both primary and secondary organic aerosols. The correlation between OC and EC can reflect the origin of carbonaceous fractions (Chow et al., 1996). Figure 3 shows the correlation between EC and OC concentrations during the APEC and Parade campaigns. During the APEC and Parade campaigns, the correlation coefficient during both control periods (R^2 = 0.9032) was larger than that during non-control periods (R^2 = 0.6468), indicating that OC and EC were mainly derived from the same sources during both pollution control periods, and were from different sources during the non-control periods. Li et al. (2017) reported that the residential burning of coal and open and domestic combustion of wood and crop residuals could contribute to more than 50% of total organic aerosol of the North China Plain during winter. During the control periods, it might be difficult to fully control the emission of residential burning. The slope of the OC/EC correlation during the pollution control period was 6.86, which was higher than that during the non-control period (3.97). This could be due to high levels of secondary OC (SOC) formation during the control periods, and/or the higher contribution from residential solid fuel (coal and biomass) burning (Liu et al., 2016).

Figure 3 here

Figure 4 shows the proportion of SNA in $PM_{2.5}$ ($\rho(SNA/PM_{2.5})$), the sulphur (S) oxidation ratio ($SOR = [SO_4^{2-}]/([SO_2]+[SO_4^{2-}])$), and nitrogen oxidation ratio ($NOR = [NO_3^-]/([NO_x]+[NO_3^-])$), along with $PM_{2.5}$ concentrations during the APEC (a) and Parade (b) campaigns. During APEC, the average $\rho(SNA/PM_{2.5})$ was 27%, which was significantly lower than before APEC (42%). During Parade, the average $\rho(SNA/PM_{2.5})$

was 35%, which was also significantly lower than before Parade (47%).

During the APEC campaign, the average SO_2 concentration was 11.3 μg m^{-3} before APEC, 9.5 μg m^{-3} during APEC, and 34.8 μg m^{-3} after APEC, respectively. The average NO_x concentration was 151 μg m^{-3} before APEC, 81 μg m^{-3} during APEC, and 220 μg m^{-3} after APEC, respectively. During the Parade campaign, the average SO_2 concentration during Parade was 1.6 μg m^{-3}, lower than both before Parade (2.7 μg m^{-3}) and after Parade (5.9 μg m^{-3}). The average NO_x concentration was also lower during Parade (26 μg m^{-3}), than before Parade (57 μg m^{-3}) and after Parade (63 μg m^{-3}).

During the APEC campaign, both the SOR and NOR declined gradually. The average SOR was 42%, 27%, and 17% before, during, and after APEC, respectively. The average NOR was 13%, 8%, and 5% before, during, and after APEC, respectively. SOR and NOR exhibited different patterns during the Parade campaign. The average SOR was 75%, 64%, and 55% before, during, and after Parade, respectively. The average NOR was 8%, 5%, and 8% before, during, and after Parade, respectively. The SOR was higher during the Parade campaign (64%) than during the APEC campaign (30%). For NOR, a higher average value was found during the APEC campaign (9%) than during the Parade campaign (7%).

The APEC campaign occurred during autumn and early winter, while the Parade campaign occurred during late summer and autumn. The active photochemical oxidation during the Parade campaign resulted in high SO_2-to-sulphate transformation rates, as indicated by the high SOR. In addition, the higher RH in summer favoured the heterogeneous reaction of sulphate formation (Figure 1). For NOR, the T was higher

during Parade than during APEC, which favoured the volatilization of nitric acid and ammonia from the particulate phase of nitrate.

These results indicate significant reductions of air pollution during the pollution control periods of APEC 2014 and Parade 2015. However, it is necessary to evaluate if meteorological conditions contributed to this improvement.

Figure 4 here

3.2 Variation of Air Pollutant Concentrations under Similar Meteorological Conditions

Figure S3 shows the prevalence of WD during the APEC and Parade campaigns. Figure S4 shows a time series of daily average $PM_{2.5}$ concentrations and PBL heights during the APEC and Parade campaigns. Both WS and PBL height during APEC and Parade were favourable for pollutant diffusion. Therefore, it is necessary to consider meteorological conditions when assessing the impacts of pollution control. One way to do this is to compare air pollution concentrations during periods when meteorological conditions were the same, i.e. under stable conditions (Wang et al., 2015; Zhang et al., 2009).

The days with stable meteorological conditions were determined with the method introduced in Section 3.2.1. As a result, eight days before APEC, six days during APEC, and seven days after APEC were defined as having stable meteorological conditions (Table S5).

Figure 6 shows the percentage reductions calculated by comparing the decreased average concentrations for all days during APEC to the average concentrations before

APEC in black bars, and the percentage reductions based on the days with stable meteorological conditions in red bars. For the difference between the periods during APEC and before APEC, the percentage reduction on days with stable meteorological conditions was much lower than the reduction calculated when considering all days, except for Ca and NO. This indicates that the method applied to days with stable meteorological conditions excluded part of the meteorological influence on pollutant concentrations. The average $PM_{2.5}$ concentration was 70 μg m^{-3} during APEC, which represented a 45.7% decrease compared with the concentration in the BAPEC period (129 μg m^{-3}) and a 44.4% decrease compared with the concentration in the AAPEC period (126 μg m^{-3}) (Figure S8). Changes of other pollutant concentrations on days with stable meteorological conditions during the APEC campaign are shown in Figure S8.

The standard deviations were also calculated with an error transfer formula that is described in detail in the Supplementary Information (S6). Figure 6 shows that the standard deviations of the percentage reduction based on days with stable meteorological conditions decreased significantly. For example, the standard deviation of the percentage reduction in $PM_{2.5}$ based on the days with stable meteorological conditions decreased from 39% to 26% compared with the same measurement when all days were considered. This indicates that by considering only days with stable meteorological conditions, the uncertainties associated with the percentage reduction figures were reduced and the reliability of the changes of air pollutants concentrations were improved. However, uncertainties remain within the percentage differences based

on the days with stable meteorological conditions, although the size of these uncertainties was reduced. Table S7 lists the percentage differences among the mean $PM_{2.5}$ concentrations of four periods that were randomly selected from within the non-control days of the APEC and Parade campaigns. This may be due to the limited sample size on days with stable meteorological conditions during the APEC campaign. It is therefore necessary to further quantify the meteorological influences.

Figure 6 here

3.3 Emission Reductions during APEC and Parade Based on GLM Predictions

The previous section showed that the number of days with stable meteorological conditions could be limited; it was therefore impossible to estimate quantitatively the contribution of meteorological conditions to the reduction of air pollutant concentrations. We developed a GLM based only on meteorological parameters to meet this requirement.

3.3.1 Model Performance and Cross-Validation Test

Figure 7 shows the scatter plot and correlation between the GLM-predicted and observed concentrations of air pollutants transformed to a natural log. Figure 8 demonstrates the time series of the observed pollutant and GLM-predicted pollutant concentrations, which displayed a good correlation. The R^2 values of the linear regression equations ranged from 0.6638 to 0.8542, most of them are higher than 0.7 except for Zn and Mn, indicating that the GLM-predicted concentrations correlated well with the observed concentrations. Specifically, the R^2 value of the linear regression

388 equation for $PM_{2.5}$ is as high as 0.8154.

389 Figure 7 here

390 Figure 8 here

391 Before applying the GLM to predict the air pollutant concentrations, the cross-
392 validation (CV) method was used to evaluate the performance of the $PM_{2.5}$ model, with
393 the assumption that it was representative of all air pollutants. The data input to the $PM_{2.5}$
394 model was allocated randomly into five equal periods, namely CV1, CV2, CV3, CV4,
395 and CV5. For each test, one period was removed from the input data and the remaining
396 data were applied to establish the CV model, which was then used to predict the $PM_{2.5}$
397 concentrations for the removed period. After five rounds, all input data were included
398 in the CV test. Figure 9 shows the time series of the observed and CV-predicted $PM_{2.5}$
399 concentrations, which demonstrates a good performance for the $PM_{2.5}$ GLM.

400 Figure 9 here

401 Table 5 shows the CV-predicted $PM_{2.5}$ concentrations. The adjusted R^2 values
402 for the five CV periods ranged from 0.710 to 0.807, which was lower than the value
403 (0.808) derived from the $PM_{2.5}$ model, due to the lack of input data. The observed mean
404 $PM_{2.5}$ concentrations were 94, 59, 44, 54, and 41 $\mu g\ m^{-3}$ for the five CV periods,
405 respectively. The corresponding CV-predicted mean $PM_{2.5}$ concentrations were 82, 57,
406 52, 65, and 47 $\mu g\ m^{-3}$, respectively. The relative error (RE) between the observed mean
407 $PM_{2.5}$ concentrations and the CV-predicted mean $PM_{2.5}$ concentrations ranged from −17%
408 to 15%, with a mean RE of −5%. The RMSE of the RE was 14.6%, reflecting the
409 uncertainties of the GLM method in quantitatively estimating the contribution of the

meteorological conditions to the air pollutant concentrations.

Table 5 also lists the daily RMSE for each CV period and the total RMSE. The daily RMSE for each CV period was calculated with the daily average $PM_{2.5}$ concentrations during each CV period, and the total RMSE was calculated with the daily average $PM_{2.5}$ concentration throughout all five CV periods combined. The daily RMSE ranged from 19 to 53 μg m^{-3}, and the total RMSE was 33 μg m^{-3}, indicating that the model prediction accuracy at the daily level needs to be improved. Liu et al. (2012) used a generalized additive model (GAM) to predict $PM_{2.5,}$ which had a total daily RMSE of 23 μg m^{-3}. Compared with their results, the CV performance in our study was satisfactory considering that the independent variables in our model were only based on meteorological parameters, while the model of Liu et al. (2012) included AOD.

The relative error calculated with the CV method for GLM was −5% (Table 5), which was smaller than the mean percentage difference (−16%) calculated based on days with stable meteorological conditions (Table S7). Moreover, the RMSE of relative error calculated with the CV method for GLM (Table 5) was 14.6%, which was also smaller than the RMSE of percentage difference (18%) calculated based on days with stable meteorological conditions (Table S7).

These indicate that the GLM reduced uncertainties of the method in quantitatively estimating the contribution of the meteorological conditions to the pollutant concentrations.

3.3.2 Model Description

Table 6 shows the concentrations of air pollutants for the GLM with adjusted R^2 values higher than 0.6. The adjusted R^2 of the $PM_{2.5}$, NO_3^-, NH_4^+, and SO_2 models are higher than 0.8, indicating that these models could explain more than 80% of the variation in air pollutant concentrations.

Again, we used the $PM_{2.5}$ model as an example. Table 7 lists the output indexes of the $PM_{2.5}$ GLM, including a model summary, analysis of variance (ANOVA), coefficients, and other indexes. The values of R, R^2, and adjusted R^2 were 0.910, 0.828, and 0.808, respectively, indicating that the $PM_{2.5}$ model can explain 80.8% of the variability of the daily average $PM_{2.5}$ concentrations. The model was statistically significant according to the p-value (<0.05) from an F-test, and the meteorological parameters eventually selected as the independent variables of the model were statistically significant according to the p-values (<0.05) from a t-test. The meteorological parameters eventually included in the model were lnWS, $lnWS_{max(lag)}$, PBL_{max}, PREC, $ln\Delta T_{(lag)}$, WS_{mode}, $WD/WS_{(lag)}$, $PBL_{min(lag)}$, $PREC_{(lag)}$, and SLP_{min}. According to the collinearity statistics, all the VIF values were within 5 and tolerance values were larger than 0.1, indicating that no serious multicollinearity existed between the independent parameters. The Durbin–Watson value (1.910) was close to 2, accounting for the good independence of the variance. Figure S9 shows the graphic residual analysis of the $PM_{2.5}$ GLM.

Table 8 summarizes the meteorological parameters included in the models and their influence on pollutant concentrations. As a result, PBL, $WS_{(lag)}$, $PREC_{(lag)}$, PREC,

and WS are included in the models more frequently, accounting for 13, 9, 8, 7, and 7 times. This indicates that these parameters have important influence on pollutant concentrations, especially for PBL included in all of the models. The parameters of the previous day also have important influence on pollutant concentrations, i.e. $WS_{(lag)}$, $PREC_{(lag)}$, $PBL_{(lag)}$, $RH_{(lag)}$, $T_{(lag)}$, $WD/WS_{(lag)}$, and $WD_{(lag)}$. Meteorological parameters have different influence on pollutant concentrations (Table 8). For example, PBL, $WS_{(lag)}$, and $PREC_{(lag)}$ represent the negative correlation with pollutant concentrations. This may be because the higher values of these meteorological parameters are in favour of pollution diffusion. On the contrary, RH, T, $WD/WS_{(lag)}$, and WD represent the positive correlation with pollutant concentrations, because the higher values of these meteorological parameters are beneficial for pollution formation and accumulation.

3.3.3 Quantitative Estimates of the Contribution of Meteorological Conditions to Air Pollutant Concentrations

We applied the GLM to predict air pollutant concentrations during APEC 2014 and Parade 2015 based on meteorological parameters. The difference between the observed and GLM-predicted concentrations was attributed to emission reduction through the implementation of air pollution control strategies.

Table 9 lists the percentage differences between the observed and GLM-predicted concentrations of air pollutants during APEC and Parade. The mean concentrations of the observed and predicted $PM_{2.5}$ were 48 and 67 μg m^{-3} during APEC, i.e. a 28% difference. The mean concentrations of the observed and predicted $PM_{2.5}$ were 15 and 20 μg m^{-3} during Parade, i.e. a 25% difference. These differences are attributed to the

emission reduction through the implementation of air pollution control strategies. As described in Section 3.1, during APEC and Parade, the mean concentrations of $PM_{2.5}$ decreased by 58% and 63% compared with before APEC and Parade. Therefore, the meteorological conditions and pollution control strategies contributed 30% and 28% to the reduction of the $PM_{2.5}$ concentration during APEC 2014, and 38% and 25% during Parade 2015, based on the assumption that the concentrations of air pollutants are only determined by meteorological conditions and emission intensities.

The emission reduction during APEC in this study is comparable to the results of other studies where meteorological influences were considered. For example, the $PM_{2.5}$ concentration decreased by 33% under the same weather conditions during APEC in Beijing as modelled by the Weather Research and Forecasting model and Community Multiscale Air Quality (WRF/CMAQ) model (Wu et al., 2015). In addition, emission control implemented in Beijing during APEC resulted in a 22% reduction in the $PM_{2.5}$ concentration, as modelled by WRF-Chem (Guo et al., 2016).

Same as $PM_{2.5}$, the differences listed in Table 9 for other pollutants show the reduction in emission of these pollutants and/or their precursors. The differences for EC were 37% (from 2.7 to 1.7 μg m^{-3}) during APEC and 33% (from 1.2 to 0.8 μg m^{-3}) during Parade. In contrast, the differences for OC were 11% (from 12.6 to 11.2 μg m^{-3}) during APEC and 8% (from 3.7 to 4.0 μg m^{-3}) during Parade. The differences for carbonaceous components (OC + EC) were 16% (from 15.3 to 12.9 μg m^{-3}) during APEC and 2% (from 4.9 to 4.8 μg m^{-3}) during Parade. This indicates that the emission reduction for OC and its precursors were smaller than the reduction of EC during APEC

and Parade. This may be because OC can originate from both primary emission and secondary transformation. The slope of the OC/EC correlation during the pollution control period reached 6.86 (Figure 3), indicating the higher levels of secondary OC (SOC) formation during the control periods.

Table 9 also shows the differences for sulphate were 44% (from 2.7 to 3.9 μg m^{-3}) during APEC and 50% (from 5.2 to 2.6 μg m^{-3}) during Parade. The differences for nitrate were 44% (from 19.0 to 10.6 μg m^{-3}) during APEC and 56% (from 3.4 to 1.5 μg m^{-3}) during Parade. The differences for ammonium were 13% (from 5.5 to 4.8 μg m^{-3}) during APEC and 38% (from 2.4 to 1.5 μg m^{-3}) during Parade. In total, the differences for SNA were 29% (from 27.2 to 19.3 μg m^{-3}) during APEC and 49% (from 11.0 to 5.6 μg m^{-3}) during Parade. The control of the SNA concentration was very effective during APEC and Parade, leading to a significant decrease of $PM_{2.5}$ during both events. The significant differences for sulphate and nitrate may indicate the control of coal combustion and/or vehicle emission were effective during APEC and Parade.

The concentration of sulphate is determined by primary emissions and secondary transformation from SO_2; thus, the changes in sulphate concentrations may not well reflect the effectiveness of emission control strategies. One needs to also include the changes in SO_2 concentrations. By adding the molar concentrations of SO_2 and SO_4^{2-} ($S = [SO_2] + [SO_4^{2-}]$), the concentration of total S was calculated. Table 9 shows the differences for SO_2 were 50% (from 6.59 to 3.32 ppb) during APEC and 2% (from 0.56 to 0.57 ppb) during Parade, while the differences for total S were 41% (from 0.322 to 0.189 μmol m^{-3}) during APEC and 33% (from 0.079 to 0.053 μmol m^{-3}) during Parade.

Coal combustion emissions is the major contributor to total S, this demonstrates the effective control of coal combustion during both APEC 2014 and Parade 2015. The difference for SO_2 during APEC was larger than that during Parade, while the difference for sulphate during Parade was larger than that during APEC. As discussed in Section 3.1, the mean SOR was 27% and 64% during APEC and Parade, respectively, indicating that the SO_2-to-sulphate transformation rate during APEC (autumn and early winter) was much lower than during Parade (late summer and autumn).

Table 9 shows NO_x and other $PM_{2.5}$ components also had significant emission reduction during APEC 2014 and Parade 2015. The differences between the observed and GLM-predicted concentrations of NO_x were 56% (from 102 to 45 ppb) during APEC and 35% (from 20 to 13 ppb) during Parade. The differences for Cl^- were 20% (from 2.58 to 2.06 μg m^{-3}) during APEC and 6% (from 0.17 to 0.16 μg m^{-3}) during Parade. The differences for K^+ were 37% (from 1.03 to 0.65 μg m^{-3}) during APEC and 25% (from 0.24 to 0.18 μg m^{-3}) during Parade. The differences for Pb, Zn, and Mn ranged from 21% to 53% during APEC and Parade. The concentrations of Cl^- have been found to be high in the fine particles produced from coal combustion (Takuwa et al., 2006), while the concentrations of K^+ are high in particles derived from combustion activities, e.g. biomass burning and coal combustion. Lead is typically considered to be a marker of emissions from coal combustion, power stations, and metallurgical plants (Dan et al., 2004; Mukai et al., 2001; Schleicher et al., 2011). Zinc can be produced by the action of a car braking and by tire wearing (Cyrys et al., 2003; Sternbeck et al., 2002). Manganese mainly originates from industrial activities. Major sources of NO_x

emissions include power plants, industry, and transportation (Liu and Zhu, 2013). The differences for the concentrations of total S, Cl^-, K^+, Pb, Zn, Mn, and NO_x, indicate that the control of anthropogenic emissions, especially coal combustion, was very effective during APEC and Parade.

3.3.4 Uncertainties of the GLM

In this study, the uncertainties of the GLM when estimating the contributions of meteorological conditions and pollution control strategies in reducing air pollution were assessed with the method of cross-validation test (Table 5) in Section 3.3.1. All the GLMs were developed following the same procedure, thus the $PM_{2.5}$ model was used as an example representative of all the pollutants. As a result, the relative error between the observed mean $PM_{2.5}$ concentrations and the CV-predicted mean $PM_{2.5}$ concentrations were within ±20%, averaging with −5%. This indicates that the $PM_{2.5}$ concentrations could be predicted with the GLM based on the meteorological conditions. The uncertainties of the GLM could refer to the RMSE of relative error for GLM of 14.6% (Table 5). It should be mentioned that the data input to the $PM_{2.5}$ model was allocated randomly into several periods, thus the RMSE of relative error for GLM would vary accordingly. In the future, we could test the uncertainties of the GLMs for other pollutants with the CV test.

4 Conclusions

During the pollution control periods of APEC 2014 and Parade 2015, the concentrations of air pollutants except ozone decreased dramatically compared with the

561 concentrations during non-control periods, accompanied by meteorological conditions
562 favourable for pollutant dispersal.

563 To estimate the contributions of meteorological conditions and pollution control
564 strategies in reducing air pollution, comparing the concentrations of air pollutants
565 during days with stable meteorological conditions is a useful method, but has limitation
566 due to high uncertainty and lack of a sufficient number of days with stable
567 meteorological conditions

568 Our study shows that, if including the nonlinear relationship between
569 meteorological parameters and air pollutant concentrations, GLMs based only on
570 meteorological parameters could provide a good explanation of the variation of
571 pollutant concentrations, with adjusted R^2 values mostly larger than 0.7. Since the
572 GLMs contained no parameters dependent on air pollution levels as independent
573 variables, they could be used to estimate the contributions of meteorological conditions
574 and pollution control strategies to the air pollution levels during emission control
575 periods.

576 With the GLMs method, we found meteorological conditions and pollution control
577 strategies played almost equally important roles in reducing air pollution in megacity
578 Beijing during APEC 2014 and Parade 2015, e.g. 30% and 28% to the reduction of the
579 $PM_{2.5}$ concentration during APEC 2014, as well as 38% and 25% during Parade 2015.
580 We also found that the control of the SNA concentration was more effective than
581 carbonaceous components. The differences between the observed and GLM-predicted
582 concentrations of specific pollutants (Cl^-, K^+, Pb, Zn, Mn, NO_x, and S) related to coal

combustion and industrial activities revealed the effective control of anthropogenic emissions.

In the future, combining the methods of source apportionment, the contributions of emission reductions for different sources in reducing air pollution could be estimated, enabling further analysis of pollution control strategies.

Data availability. The data of stationary measurements are available upon requests.

Author contribution. T. Zhu and P. F. Liang designed the experiments. P. F. Liang collected and weighed the $PM_{2.5}$ filter samples. P. F. Liang, Y. H. Fang, Y. Q. Han, and J. X. Wang carried out the analysis of the components in $PM_{2.5}$. Y. S. Wu and M. Hu provided the data of gaseous pollutant concentrations. Y. R. Li computed the data of planetary boundary layer heights from GDAS and P. F. Liang developed the GLM. J. X. Wang managed the data. P. F. Liang analyzed the data with contributions from all co-authors. P. F. Liang prepared the manuscript with helps from T. Zhu.

Acknowledgement. This study was supported by the National Natural Science Foundation Committee of China (41421064, 21190051), the European 7th Framework Programme Project PURGE (265325), and the Collaborative Innovation Center for Regional Environmental Quality.

Reference

Barmpadimos, I., Keller, J., Oderbolz, D., Hueglin, C., and Prevot, A. S. H.: One decade of parallel fine ($PM_{2.5}$) and coarse (PM_{10}-$PM_{2.5}$) particulate matter measurements

in Europe: trends and variability, Atmos. Chem. Phys., 12, 3189-3203, doi:10.5194/acp-12-3189-2012, 2012.

Calkins, C., Ge, C., Wang, J., Anderson, M., and Yang, K.: Effects of meteorological conditions on sulfur dioxide air pollution in the North China Plain during winters of 2006–2015. Atmos. Environ., 147, 296-309, doi:10.1016/j.atmosenv.2016.10.005, 2016.

CEPB: Chengdu Environmental Protection Bureau, available at: http://www.cdepb.gov.cn/cdepbws/Web/Template/GovDefaultInfo.aspx?cid=236&aid=22738 (last assess: 25 May 2017), (in Chinese), 2013.

China, S. C. o., State Council of P. R. China's notification on Action Plan for Air Pollution Prevention and Control. 2013.

Chitranshi, S., Sharma, S. P., and Dey, S.: Spatio-temporal variations in the estimation of PM_{10} from MODIS-derived aerosol optical depth for the urban areas in the Central Indo-Gangetic Plain, Meteorol. Atmos. Phys., 127, 107-121, doi:10.1007/s00703-014-0347-z, 2015.

Chow, J. C., Watson, J. G., Lu, Z. Q., Lowenthal, D. H., Frazier, C. A., Solomon, P. A., Thuillier, R. H., and Magliano, K.: Descriptive analysis of $PM_{2.5}$ and PM_{10} at regionally representative locations during SJVAQS/AUSPEX, Atmos. Environ., 30, 2079-2112, doi 10.1016/1352-2310(95)00402-5, 1996.

Chudnovsky, A. A., Koutrakis, P., Kloog, I., Melly, S., Nordio, F., Lyapustin, A., Wang, Y. J., and Schwartz, J.: Fine particulate matter predictions using high resolution Aerosol Optical Depth (AOD) retrievals, Atmos. Environ., 89, 189-198, doi:10.1016/j.atmosenv.2014.02.019, 2014.

Cyrys, J., Heinrich, J., Hoek, G., Meliefste, K., Lewne, M., Gehring, U., Bellander, T., Fischer, P., Van Vliet, P., Brauer, M., Wichmann, H. E., and Brunekreef, B.: Comparison between different traffic-related particle indicators: Elemental carbon (EC), $PM_{2.5}$ mass, and absorbance, J. Expo. Anal. Env. Epid., 13, 134-143, doi:10.1038/sj.jea.7500262, 2003.

Dan, M., Zhuang, G. S., Li, X. X., Tao, H. R., and Zhuang, Y. H.: The characteristics of carbonaceous species and their sources in $PM_{2.5}$ in Beijing, Atmos. Environ., 38, 3443-3452, doi:10.1016/j.atmosenv.2004.02.052, 2004.

Diaz-Robles, L. A., Ortega, J. C., Fu, J. S., Reed, G. D., Chow, J. C., Watson, J. G., and Moncada-Herrera, J. A.: A hybrid ARIMA and artificial neural networks model to forecast particulate matter in urban areas: The case of Temuco, Chile, Atmos. Environ., 42, 8331-8340, doi:10.1016/j.atmosenv.2008.07.020, 2008.

GEPB: Guangzhou Environmental Protection Bureau, available at: http://www.gz.gov.cn/gzgov/s2812/200912/163197.shtml (last assess: 25 May 2017), (in Chinese), 2009.

Guo, J. P., He, J., Liu, H. L., Miao, Y. C., Liu, H., and Zhai, P. M.: Impact of various

emission control schemes on air quality using WRF-Chem during APEC China 2014, Atmos. Environ., 140, 311-319, doi:10.1016/j.atmosenv.2016.05.046, 2016.

Han, T. T., Xu, W. Q., Chen, C., Liu, X. G., Wang, Q. Q., Li, J., Zhao, X. J., Du, W., Wang, Z. F., and Sun, Y. L.: Chemical apportionment of aerosol optical properties during the Asia-Pacific Economic Cooperation summit in Beijing, China, J. Geophys. Res., 120, doi:10.1002/2015JD023918, 2015.

Hien, P. D., Bac, V. T., Tham, H. C., Nhan, D. D., and Vinh, L. D.: Influence of meteorological conditions on $PM_{2.5}$ and $PM_{2.5-10}$ concentrations during the monsoon season in Hanoi, Vietnam, Atmos. Environ., 36, 3473-3484, doi:10.1016/S1352-2310(02)00295-9, 2002.

Huang, X. F., He, L. Y., Hu, M., Canagaratna, M. R., Sun, Y., Zhang, Q., Zhu, T., Xue, L., Zeng, L. W., Liu, X. G., Zhang, Y. H., Jayne, J. T., Ng, N. L., and Worsnop, D. R.: Highly time-resolved chemical characterization of atmospheric submicron particles during 2008 Beijing Olympic Games using an Aerodyne High-Resolution Aerosol Mass Spectrometer, Atmos. Chem. Phys., 10, 8933-8945, doi:10.5194/acp-10-8933-2010, 2010.

Huang, X. F., He, L. Y., Xue, L., Sun, T. L., Zeng, L. W., Gong, Z. H., Hu, M., and Zhu, T.: Highly time-resolved chemical characterization of atmospheric fine particles during 2010 Shanghai World Expo, Atmos. Chem. Phys., 12, 4897-4907, doi:10.5194/acp-12-4897-2012, 2012.

Kelly, F. J. and Zhu, T.: Transport solutions for cleaner air, Science, 352, 934-936, doi:10.1126/science.aaf3420, 2016.

Liu, H., Wang, X. M., Zhang, J. P., He, K. B., Wu, Y., and Xu, J. Y.: Emission controls and changes in air quality in Guangzhou during the Asian Games, Atmos. Environ., 76, 81-93, doi:10.1016/j.atmosenv.2012.08.004, 2013.

Li, H., Zhang, Q., Zhang, Q., Chen, C., Wang, L., Wei, Z., Zhou, S., Parworth, C., Zheng, B., and Canonaco, F.: Wintertime aerosol chemistry and haze evolution in an extremely polluted city of the North China Plain: significant contribution from coal and biomass combustion, Atmos. Chem. Phys., 17, 1-31, doi:10.5194/acp-17-4751-2017, 2017.

Liu, J., Mauzerall, D. L., Chen, Q., Zhang, Q., Song, Y., Peng, W., Klimont, Z., Qiu, X. H., Zhang, S. Q., Hu, M., Lin, W. L., Smith, K. R., and Zhu, T.: Air pollutant emissions from Chinese households: A major and underappreciated ambient pollution source, P. Natl. Acad. Sci. USA., 113, 7756-7761, doi: 10.1073/pnas.1604537113, 2016.

Liu, J., and Zhu, T.: NO_x in Chinese Megacities, Nato. Sci. Peace. Secur., 120, 249-263, doi:10.1007/978-94-007-5034-0_20, 2013.

Liu, W., Li, X. D., Chen, Z., Zeng, G. M., Leon, T., Liang, J., Huang, G. H., Gao, Z. H., Jiao, S., He, X. X., and Lai, M. Y.: Land use regression models coupled with

meteorology to model spatial and temporal variability of NO_2 and PM_{10} in Changsha, China, Atmos. Environ., 116, 272-280, doi:10.1016/j.atmosenv.2015.06.056, 2015.

Liu, Y., Franklin, M., Kahn, R., and Koutrakis, P.: Using aerosol optical thickness to predict ground-level $PM_{2.5}$ concentrations in the St. Louis area: A comparison between MISR and MODIS, Remote. Sens. Environ., 107, 33-44, doi:10.1016/j.rse.2006.05.022, 2007.

Liu, Y., He, K. B., Li, S. S., Wang, Z. X., Christiani, D. C., and Koutrakis, P.: A statistical model to evaluate the effectiveness of $PM_{2.5}$ emissions control during the Beijing 2008 Olympic Games, Environ. Int., 44, 100-105, doi:10.1016/j.envint.2012.02.003, 2012.

Mukai, H., Tanaka, A., Fujii, T., Zeng, Y. Q., Hong, Y. T., Tang, J., Guo, S., Xue, H. S., Sun, Z. L., Zhou, J. T., Xue, D. M., Zhao, J., Zhai, G. H., Gu, J. L., and Zhai, P. Y.: Regional characteristics of sulfur and lead isotope ratios in the atmosphere at several Chinese urban sites, Environ. Sci. Technol., 35, 1064-1071, doi:10.1021/es001399u, 2001.

Mustaffa, N. I. H., Latif, M. T., Ali, M. M., and Khan, M. F.: Source apportionment of surfactants in marine aerosols at different locations along the Malacca Straits, Environ. Sci. Pollut. R., 21, 6590-6602, doi:10.1007/s11356-014-2562-z, 2014.

Nguyen, T. T. N., Bui, H. Q., Pham, H. V., Luu, H. V., Man, C. D., Pham, H. N., Le, H. T., and Nguyen, T. T.: Particulate matter concentration mapping from MODIS satellite data: a Vietnamese case study, Environ. Res. Lett., 10, 095016, doi:10.1088/1748-9326/10/9/095016, 2015.

NOAA Air Resources Laboratory: http://ready.arl.noaa.gov/READYamet.php/.

Raman, R. S. and Kumar, S.: First measurements of ambient aerosol over an ecologically sensitive zone in Central India: Relationships between $PM_{2.5}$ mass, its optical properties, and meteorology, Sci. Total. Environ., 550, 706-716, doi:10.1016/j.scitotenv.2016.01.092, 2016.

Richmond-Bryant, J., Saganich, C., Bukiewicz, L., and Kalin, R.: Associations of $PM_{2.5}$ and black carbon concentrations with traffic, idling, background pollution, and meteorology during school dismissals, Sci. Total. Environ., 407, 3357-3364, doi:10.1016/j.scitotenv.2009.01.046, 2009.

Schleicher, N., Norra, S., Dietze, V., Yu, Y., Fricker, M., Kaminski, U., Chen, Y., and Cen, K.: The effect of mitigation measures on size distributed mass concentrations of atmospheric particles and black carbon concentrations during the Olympic Summer Games 2008 in Beijing, Sci. Total. Environ., 412, 185-193, doi:10.1016/j.scitotenv.2011.09.084, 2011.

SEPB: Shanghai Environmental Protection Bureau, available at: http://www.sepb.gov.cn/fa/cms/shhj//shhj2272/shhj2159/2010/02/20671.htm (last

721 assess: 25 May 2017), (in Chinese), 2010.
722 Sotoudeheian, S. and Arhami, M.: Estimating ground-level PM_{10} using satellite remote
723 sensing and ground-based meteorological measurements over Tehran, J. Environ.
724 Health. Sci., 12, 122, doi:10.1186/S40201-014-0122-6, 2014.
725 Sternbeck, J., Sjodin, A., and Andreasson, K.: Metal emissions from road traffic and
726 the influence of resuspension-results from two tunnel studies, Atmos. Environ., 36,
727 4735-4744, doi:10.1016/S1352-2310(02)00561-7, 2002.
728 Takuwa, T., Mkilaha, I. S. N., and Naruse, I.: Mechanisms of fine particulates formation
729 with alkali metal compounds during coal combustion, Fuel, 85, 671-678,
730 doi:10.1016/j.fuel.2005.08.043, 2006.
731 Tao, J., Gao, J., Zhang, L., Zhang, R., Che, H., Zhang, Z., Lin, Z., Jing, J., Cao, J., and
732 Hsu, S. C.: $PM_{2.5}$ pollution in a megacity of southwest China: source
733 apportionment and implication, Atmos. Chem. Phys., 14, 8679-8699,
734 doi:10.5194/acp-14-8679-2014, 2014.
735 Tian, J. and Chen, D. M.: A semi-empirical model for predicting hourly ground-level
736 fine particulate matter ($PM_{2.5}$) concentration in southern Ontario from satellite
737 remote sensing and ground-based meteorological measurements, Remote. Sens.
738 Environ., 114, 221-229, doi:10.1016/j.rse.2009.09.011, 2010.
739 Wang, Z. S., Li, Y. T., Chen, T., Li, L. J., Liu, B. X., Zhang, D. W., Sun, F., Wei, Q.,
740 Jiang, L., and Pan, L. B.: Changes in atmospheric composition during the 2014
741 APEC conference in Beijing, J. Geophys. Res., 120, 12695-12707,
742 doi:10.1002/2015JD023652, 2015.
743 Wen, W., Cheng, S., Chen, X., Wang, G., Li, S., Wang, X., and Liu, X.: Impact of
744 emission control on PM and the chemical composition change in Beijing-Tianjin-
745 Hebei during the APEC summit 2014, Environ. Sci. Pollut. R., 23, 4509-4521,
746 doi:10.1007/s11356-015-5379-5, 2016.
747 Wu, Q., Xu, W., and Wang, Z.: The air quality forecast about $PM_{2.5}$ before and during
748 APEC 2014 in Beijing by WRF-CMAQ model system, EGU General Assembly
749 Conference, 2015.
750 Yanosky, J. D., Paciorek, C. J., Laden, F., Hart, J. E., Puett, R. C., Liao, D. P., and Suh,
751 H. H.: Spatio-temporal modeling of particulate air pollution in the conterminous
752 United States using geographic and meteorological predictors, Environ. Health.,
753 13, 63, doi:10.1186/1476-069x-13-63, 2014.
754 You, W., Zang, Z. L., Pan, X. B., Zhang, L. F., and Chen, D.: Estimating $PM_{2.5}$ in Xi'an,
755 China using aerosol optical depth: A comparison between the MODIS and MISR
756 retrieval models, Sci. Total. Environ., 505, 1156-1165,
757 doi:10.1016/j.scitotenv.2014.11.024, 2015.
758 Zhang, J. P., Zhu, T., Zhang, Q. H., Li, C. C., Shu, H. L., Ying, Y., Dai, Z. P., Wang, X.,
759 Liu, X. Y., Liang, A. M., Shen, H. X., and Yi, B. Q.: The impact of circulation

patterns on regional transport pathways and air quality over Beijing and its surroundings, Atmos. Chem. Phys., 12, 5031-5053, doi:10.5194/acp-12-5031-2012, 2012.

Zhang, X. Y., Wang, Y. Q., Lin, W. L., Zhang, Y. M., Zhang, X. C., Gong, S., Zhao, P., Yang, Y. Q., Wang, J. Z., Hou, Q., Zhang, X. L., Che, H. Z., Guo, J. P., and Li, Y.: Changes of atmospheric composition and optical properties over Beijing 2008 Olympic monitoring campaign, B. Am. Meteorol. Soc., 90, 1633, doi:10.1175/2009BAMS2804.1, 2009.

Zhang, W., Zhu, T., Yang, W., Bai, Z., Sun, Y. L., Xu, Y., Yin, B., and Zhao, X.: Airborne measurements of gas and particle pollutants during CAREBeijing-2008, Atmos. Chem. Phys., 14, 301-316, doi:10.5194/acp-14-301-2014, 2014.

Figure Captions:

Figure 1. Time series of atmospheric particulate matter of aerodynamic diameter ≤ 2.5 μm ($PM_{2.5}$) and the concentrations of its components, wind direction (WD), wind speed (WS), temperature (T), and relative humidity (RH) before, during, and after (a) APEC 2014 and (b) Parade 2015. The blue-shaded areas highlight the pollution control periods of APEC 2014 (3 November to 12 November 2014) and Parade 2015 (20 August to 3 September 2015).

Figure 2. Proportions of the measured components in $PM_{2.5}$ during (a) APEC 2014 and (b) Parade 2015 campaigns, including organic carbon (OC), elemental carbon (EC), SO_4^{2-}, NO_3^-, NH_4^+, Cl^- and elements. BAPEC/BParade: before APEC/Parade, AAPEC/AParade: after APEC/Parade.

Figure 3. Scatter plot and correlations between organic carbon (OC: *y*-axis) and elemental carbon (EC: *x*-axis) concentrations of $PM_{2.5}$ during the APEC 2014 and Parade 2015 campaigns. The red symbols denote the non-control period and the black symbols denote the pollution control period. The linear regression equations and R^2 values are given for these two campaigns.

Figure 4. Upper panel: time series of the proportion of sulphate, nitrate, and ammonia (SNA) in $PM_{2.5}$ ($\rho(SNA/PM_{2.5})$) and $PM_{2.5}$ mass concentrations (the black bar represents $PM_{2.5}$ concentration and the red line represents $\rho(SNA/PM_{2.5})$). Middle panel: SO_2, SO_4^{2-}, and SOR ($[SO_4^{2-}]/([SO_2]+[SO_4^{2-}])$). Lower panel: NO_x, NO_3^-, and NOR

795 ($[NO_3^-]/([NO_x]+[NO_3^-])$). Data collected during the (a) APEC 2014 and (b) Parade
796 2015 campaigns. The hollow bars represent gaseous pollutants (red for SO_2, blue for
797 NO_x), and solid bars represent secondary inorganic ions (red for sulphate, blue for
798 nitrate).
799
800 Figure 5. Scatter plot showing the correlation between daily $PM_{2.5}$ concentrations (*y*-
801 axis) and (a) daily PBL heights (*x*-axis) and (b) daily WSs (*x*-axis) during the sampling
802 periods. The red and black scattered points represent different distribution areas. The
803 piecewise function regression equations and the corresponding values of PBL height
804 and WS according to the intersections are given.
805
806 Figure 6. The percentage reductions of pollutant concentrations under similar
807 meteorological conditions. The black bars represent the percentage reductions
808 calculated by comparing the decreased average concentrations during APEC to the
809 average concentrations before APEC. The red bars represent the percentage reductions
810 calculated by comparing the decreased average concentrations during APEC to the
811 average concentrations before APEC based only on the days with stable meteorological
812 conditions. The whiskers represent the standard deviations of the percentage reductions.
813
814 Figure 7. Scatter plot and correlations between GLM-predicted (*y*-axis) and observed
815 (*x*-axis) concentrations of pollutants transformed to a natural log. The linear regression
816 equations and R^2 values are given.
817

818 Figure 8. Time series of the observed (in black line) and GLM-predicted pollutant
819 concentrations (in red line).
820
821 Figure 9. Time series of the observed and cross-validation (CV) predicted $PM_{2.5}$
822 concentrations during five CV periods. The black line represents the observed $PM_{2.5}$
823 concentration and the red line represents the CV-predicted $PM_{2.5}$ concentration.
824
825
826

827 Table 1. Summary of statistical models applied to predict air pollutant concentrations
828 with meteorological parameters.

Dependent variables	Independent variables	R^2	Methods[1]	Applications
$PM_{2.5}$	meteorological parameters (T/RH/PBL/WS/cloud fraction), AOT	0.47	MLR	Gupta and Christopher, 2009
PM_{10}	meteorological parameters (T/WD/RH/PBL/WS), AOD	0.21/0.30 (MODIS/MISR[2])	MLR	Sotoudeheian and Arhami, 2014
PM_{10}	meteorological parameters (RH/WS/T), AOD	0.49-0.88 (spatial-temporal variability)	MLR	Chitranshi et al., 2015
$PM_{2.5}$	meteorological parameters (T/RH/PREC), AOT	0.60/0.58 (MOD/MYD[3])	MLR	Nguyen et al., 2015
ln($PM_{2.5}$), ln($PM_{2.5-10}$)	meteorological parameters (ln(PREC)/ln(RH)/ln(WS)/ln(SUN)/ln(T)), atmospheric turbulence parameters (ln($\Delta u/\Delta z$)/ln($\Delta\theta/\Delta z$))	0.60-0.74	GLM	Hien et al., 2002
ln($PM_{2.5}$)	meteorological parameters (T/WD/ln(WS)/ln(PBL)), ln(AOT), categorical parameters	0.51/0.62 (MODIS/MISR)	GLM	Liu et al., 2007
log($PM_{2.5}$), log(BC)	meteorological parameters (T/wind index), traffic-related parameters	0.62/0.42 ($PM_{2.5}$/BC)	GLM	Richmond-Bryant et al., 2009
ln($PM_{2.5}$)	meteorological parameters (ln(PBL)/GEO-4 RH/ln(surface RH)/T), ln(AOD)	0.65	GLM	Tian and Chen, 2010
ln(PM_{10})	meteorological parameters (T/WD/RH/ln(PBL)/ln(WS)), ln(AOD)	0.18/0.38 (MODIS/MISR)	GLM	Sotoudeheian and Arhami, 2014
ln($PM_{2.5}$)	meteorological parameters (ln(PBL)/RH/Vis/ln(T)/ln(WS)), ln(AOD)	0.67/0.72 (MODIS/MISR)	GLM	You et al., 2015
ln($PM_{2.5}$)	meteorological parameters (WS/WD/T/RH/pressure), optical properties (absorption/scattering/attenuation co-efficient)	0.54/0.31/0.32/0.88 (winter/pre-monsoon/monsoon/post-monsoon)	GLM	Raman and Kumar, 2016
PM_{10}, $PM_{2.5}$	smooth non-parametric functions of spatial/temporal variates	0.58	GAM	Barmpadimos et al., 2012
$PM_{2.5}$, PM_{10}, $PM_{2.5-10}$	smooth non-parametric functions of spatial/temporal variates	0.77/0.58/0.46-0.52 ($PM_{2.5}$/PM_{10}/$PM_{2.5-10}$)	GAM	Yanosky et al., 2014
PM_{10}	meteorological parameters (WS/T_{min}/T_{max}), previous day PM_{10}	0.78	ANN	Diaz-Robles et al., 2008
$PM_{2.5}$	meteorological parameters (WS/RH/PBL/WS*PBL), AOD, spatial	0.89	LUR	Chudnovsky et al., 2014

	explanatory variables			
PM_{10}, NO_2	meteorological parameters (T/RH/WS/air pressure/cloud cover/percentage of haze/mist/rain/sun), spatial explanatory variables	0.45/0.43 (PM_{10}/NO_2)	LUR	Liu et al., 2015

[1]MLR: multiple linear regression model, GLM: generalized linear regression model, GAM: generalized additive model, ANN: artificial neural networks, LUR: land use regression model.

[2]MODIS: Moderate resolution imaging spectroradiometer, MISR: Multi-angle imaging spectroradiometer.

[3]MOD/MYD: MODIS Terra (AM overpass) and Aqua (PM overpass).

829

830

831 Table 2. Air pollution control strategies during APEC 2014 and Parade 2015.

Periods	Control measures	Detail of measures
APEC 2014 (3 to 12 November 2014) and **Parade 2015** (20 August to 3 September 2015)	Traffic control	The odd/even plate number rule for traffic control in Beijing, Tianjin, Hebei and Shandong; 70% (APEC 2014)/80% (Parade 2015) of official vehicle and "yellow label vehicles" were banned from Beijing's roads; Trucks limited to run inside the 6th Ring Road between 6 AM to 24 PM.
	Industrial emission control	More than 10,000 factories production limited or halted in Beijing and Hebei, Tianjin, Shandong, Shanxi and Inner Mongolia which surround Beijing city.
	Dust pollution control	Dust emission factories and outdoor constructions shut down or limited in Beijing and near area; Enhancing road cleaning and spray and aspirating in Beijing.
	Coal-fired control	State-owned enterprise productions enhancing limited and 40% coal-fired boilers shut down in Beijing; more special pollutant emission factory limited around Beijing.

832

833

834 Table 3. Meteorological parameters used in the GLM in this study. The calculation of
835 each meteorological parameter is based on the sample duration of 23.5 h (09:30–09:00
836 LT the next day).

Parameters	Abbreviations	Description
Wind direction value*	WD	The average of wind direction values.
	WD_{sum}	The sum of wind direction values.
	WD_{mode}	The mode of wind direction values.
Wind speed (m s^{-1})	WS	The average of wind speed.
	WS_{mode}	The mode of wind speed.
	WS_{max}	The maximum of wind speed.
Temperature (°C）	T	The average of temperature.
	T_{max}	The maximum of temperature.
	T_{min}	The minimum of temperature.
	ΔT	The difference of temperature.
Sea level pressure (hPa)	SLP	The average of sea level pressure.
	SLP_{max}	The maximum of sea level pressure.
	SLP_{min}	The minimum of sea level pressure.
Relative humidity (%)	RH	The average of relative humidity.
	RH_{max}	The maximum of relative humidity.
Precipitation (mm)	PREC	The accumulation of precipitation.
Wind index	WD/WS	The average of wind direction value/wind speed.
	WD/WS_{sum}	The sum of wind direction value/wind speed.
Planetary boundary layer height (m)	PBL	The average of 3-h planetary boundary layer height.
	PBL_{min}	The minimum of 3-h planetary boundary layer height.
	PBL_{max}	The maximum of 3-h planetary boundary layer height.

* Since the degree data of wind direction cannot be applied directly, the values of wind directions are donated such that value = 1, 2, 3 for north, south, and “calm and variable”, respectively.

837

838 Table 4. Statistical summary showing the mean concentrations and standard deviations
839 of $PM_{2.5}$, gaseous pollutants, and $PM_{2.5}$ components. BAPEC/BParade: before
840 APEC/Parade, AAPEC/AParade: after APEC/Parade.

Pollutants	Units	BAPEC	APEC	AAPEC	BParade	Parade	AParade
$PM_{2.5}$		113±62	48±35	97±84	41±14	15±6	39±28
OC		15.3±8.7	11.2±7.2	21.3±15.5	7.4±1.9	4.0±1.0	6.3±3.1
EC		2.7±1.4	1.7±1.0	3.5±1.8	1.6±0.3	0.8±0.1	2.0±1.0
SO_4^{2-}		12.6±9.1	3.9±3.0	9.6±12.4	10.6±6.2	2.6±1.3	7.9±7.3
NO_3^-		29.4±21.4	10.6±11.0	16.3±19.4	5.0±3.9	1.5±1.5	6.4±6.2
NH_4^+		15.0±10.6	4.8±4.2	10.3±11.9	5.2±2.6	1.5±1.0	5.4±5.4
Cl^-		3.19±1.61	2.06±2.11	6.59±6.67	0.20±0.16	0.16±0.12	0.53±0.24
Na^+	μg m^{-3}	0.50±0.26	0.26±0.15	0.57±0.46	0.16±0.09	0.10±0.05	0.16±0.08
K^+		1.20±0.63	0.65±0.51	1.52±1.43	0.30±0.13	0.18±0.08	0.38±0.20
Mg^{2+}		0.07±0.03	0.09±0.02	0.13±0.07	0.01±0.01	0.01±0.00	0.02±0.01
Ca^{2+}		0.52±0.34	0.28±0.19	0.53±0.40	0.14±0.07	0.10±0.04	0.17±0.05
SO_2		11.3±5.0	9.5±6.8	34.8±15.3	2.7±1.6	1.6±1.4	5.9±5.2
NO		54.2±30.5	21.9±13.8	112.3±63.2	3.2±2.1	1.2±0.9	9.3±7.5
NO_x		151±62	81±46	220±107	57±11	26±13	63±24
O_3		23±16	38±19	17±14	116±33	79±22	74±27
Ca		582±431	591±335	1536±579	202±64	108±36	188±130
Co		0.48±0.21	0.34±0.18	0.90±0.52	0.21±0.08	0.05±0.02	0.16±0.10
Ni		3.20±1.56	5.07±7.42	5.17±2.50	1.75±1.16	0.63±0.72	1.16±0.67
Cu		35.7±16.2	19.1±12.6	43.3±31.2	12.4±5.1	3.7±1.3	9.6±6.5
Zn		320±146	128±120	315±310	97±46	20±9	71±54
Se		6.45±3.46	3.76±3.84	5.22±6.56	7.06±3.41	3.19±2.76	3.17±2.76
Mo		2.20±1.12	1.63±1.14	2.85±2.67	0.62±0.41	0.16±0.14	0.53±0.46
Cd		3.86±2.53	1.41±1.25	3.11±2.52	2.35±5.72	0.22±0.17	0.71±0.74
Tl	ng m^{-3}	1.87±0.90	0.87±1.01	2.03±1.96	0.50±0.31	0.05±0.06	0.33±0.39
Pb		121±59	55±52	104±81	36±19	9±6	29±26
Th		0.09±0.05	0.06±0.03	0.09±0.06	0.02±0.01	0.01±0.01	0.01±0.01
U		0.06±0.02	0.05±0.03	0.09±0.06	0.02±0.01	0.00±0.00	0.01±0.02
Na		529±261	355±209	907±632	182±71	96±39	181±96
Mg		153±94	105±47	236±143	43±13	15±8	24±15
Al		516±324	338±154	588±406	141±82	130±60	136±93
Mn		55.5±23.3	34.5±24.1	61.6±52.4	17.3±6.4	3.6±1.8	14.8±9.2
Fe		755±314	573±336	883±538	269±71	98±28	234±139
Ba		16.3±8.0	11.0±8.4	13.8±8.1	4.7±1.6	1.9±0.6	4.1±2.3

841
842
843
844
845

Table 5. The cross-validation (CV) performance of the $PM_{2.5}$ GLM.

Periods	Adjusted R^2	Observed mean values (μg m^{-3})	Predicted mean values (μg m^{-3})	Daily RMSE (μg m^{-3})	Total RMSE (μg m^{-3})	Relative errors (RE)*	Mean RE	RMSE of RE
CV1	0.748	94	82	53		15%		
CV2	0.798	59	57	20		4%		
CV3	0.783	44	52	19	33	-15%	-5%	14.6%
CV4	0.710	54	65	27		-17%		
CV5	0.807	41	47	30		-13%		

*Relative error (RE) = (Predicted mean value - Observed mean value)/Predicted mean value × 100%.

Table 6. The concentrations of air pollutants for the GLM with adjusted R^2 values higher than 0.6.

Pollutants	Model descriptions	Adjusted R^2
$PM_{2.5}$	$\ln(PM_{2.5})$=-0.48lnWS-0.43$lnWS_{max(lag)}$-0.00076PBL_{max}-0.11PREC+0.25ln$\Delta T_{(lag)}$-0.14WS_{mode}+0.48$WD/WS_{(lag)}$+0.0043$PBL_{min(lag)}$-0.025$PREC_{(lag)}$-0.015SLP_{min}+19.51	0.808
EC	ln(EC)=0.60lnWD/WS_{sum}-0.59lnPBL-0.017$PREC_{(lag)}$+0.22lnΔT-0.50ln$WS_{(lag)}$+0.25ln$PBL_{max(lag)}$-0.17	0.780
OC	ln(OC)= -0.44lnWS+0.47$WD/WS_{(lag)}$-0.67lnPBL-0.020$PREC_{(lag)}$+0.67lnWD+0.17lnΔT-0.65ln$RH_{max(lag)}$+7.84	0.751
SO_4^{2-}	ln(SO_4^{2-})=-0.99ln$WS_{(lag)}$+0.066T_{min}-0.040$PREC_{(lag)}$-1.20lnPBL+0.0011$PBL_{(lag)}$+0.019RH-0.12PREC+0.087WS_{max}+6.68	0.795
NO_3^-	ln(NO_3^-)=-1.90lnPBL-0.96ln$WS_{(lag)}$+0.88WD+0.0045PBL_{min}-0.20PREC+0.12WS_{max}+1.57lnRH+0.60ln$\Delta T_{(lag)}$-1.22ln$RH_{max(lag)}$-0.047ΔT+9.32	0.833
NH_4^+	ln(NH_4^+)=0.040RH-1.27ln$WS_{(lag)}$-1.03ln$RH_{(lag)}$-0.00075PBL_{max}-0.16PREC+0.33ln$\Delta T_{(lag)}$+4.28	0.813
Cl^-	ln(Cl^-)= -1.12lnPBL-0.072$T_{(lag)}$+1.60lnWD-2.32ln$RH_{max(lag)}$+0.53ln$WD/WS_{sum(lag)}$+14.69	0.737
K^+	ln(K^+)= -0.75lnPBL-0.66ln$WS_{(lag)}$-0.020$RH_{(lag)}$+0.0056PBL_{min}-0.20WS_{mode}+0.33ln$\triangle T_{(lag)}$-0.47ln$PBL_{max(lag)}$-0.087PREC+0.66lnRH+5.46	0.717
Pb	ln(Pb)= -0.61lnWS-0.67ln$WS_{max(lag)}$+0.36ln$\Delta T_{(lag)}$-0.00062PBL_{max}-0.19WS_{mode}-0.030$PREC_{(lag)}$+5.39	0.721
Zn	ln(Zn)=-0.81lnWS-0.41ln$WS_{max(lag)}$-0.0016PBL-0.36ln$WS_{mode(lag)}$+6.56	0.627
Mn	ln(Mn)=0.80WD/WS-0.98lnPBL-0.043$PREC_{(lag)}$+0.57$WD/WS_{(lag)}$-0.017RH-0.023SLP+0.0030$PBL_{min(lag)}$+31.04	0.656
SO_2	ln(SO_2)=-1.32lnPBL-0.071$PREC_{(lag)}$-0.047PREC+0.29$WD_{mode(lag)}$-0.026RH-0.47ln$WS_{(lag)}$+14.12lnSLP_{max}-87.56	0.803
NO_x	ln(NO_x)=0.014WD/WS_{sum}-0.030T_{min}+0.27lnΔT-0.44lnPBL-0.015PREC-0.012$PREC_{(lag)}$+5.30	0.772

852 Table 7. The output indexes of the $PM_{2.5}$ GLM, including a model summary, analysis
853 of variance (ANOVA), coefficients, and other indexes.

Model Summary and ANOVA						
R	R^2	Adjusted R^2	Std. Error of the Estimate	Durbin-Watson	F	Sig.*
0.910	0.828	0.808	0.411	1.910	41.763	0.000

Coefficients						
Model	Unstandardized Coefficients		t	Sig.*	Collinearity Statistics	
	B	Std. Error			Tolerance	VIF
(Constant)	19.512	6.871	2.840	0.006		
lnWS	-0.483	0.162	-2.971	0.004	0.313	3.194
$lnWS_{max(lag)}$	-0.431	0.153	-2.818	0.006	0.300	3.331
PBL_{max}	-0.001	0.000	-6.747	0.000	0.395	2.534
PREC	-0.110	0.029	-3.735	0.000	0.618	1.618
$ln\triangle T_{(lag)}$	0.247	0.083	2.975	0.004	0.662	1.512
WS_{mode}	-0.135	0.050	-2.726	0.008	0.493	2.027
$WD/WS_{(lag)}$	0.476	0.148	3.222	0.002	0.353	2.829
$PBL_{min(lag)}$	0.004	0.001	3.510	0.001	0.407	2.459
$PREC_{(lag)}$	-0.025	0.009	-2.796	0.006	0.707	1.415
SLP_{min}	-0.015	0.007	-2.176	0.032	0.707	1.414

*The significance level is 0.05.

854
855
856
857

Table 8. The influence of the meteorological parameters included in the GLMs on pollutant concentrations[1].

Parameters	Included in the GLM (times)[2]	$PM_{2.5}$	EC	OC	SO_4^{2-}	NO_3^-	NH_4^+	Cl^-	K^+	Pb	Zn	Mn	SO_2	NO_x
PBL	13	-	-	-	-	+-	-	-	+-	-	-	-	-	-
$WS_{(lag)}$	9	-	-		-	-	-		-	-	-		-	
$PREC_{(lag)}$	8	-	-	-	-					-		-	-	-
PREC	7	-			-	-	-		-				-	-
WS	7	-		-	+	+			-	-	-			
RH	6				+	+	+		+			-	-	
$PBL_{(lag)}$	5	+	+		+				-			+		
$RH_{(lag)}$	5			-		-	-	-	-					
T	5		+	+	+	+-								-+
$T_{(lag)}$	5	+					+	-	+	+				
$WD/WS_{(lag)}$	4	+		+				+				+		
SLP	3	-										-	+	
WD	3			+		+		+						
WD/WS	3		+									+		+
$WD_{(lag)}$	1												+	

[1] "+" represents the positive correlation, and "-" represents the negative correlation between meteorological parameters and pollutant concentrations.

[2]If a parameter is included in the model for several times, it will be counted as one time.

865 Table 9. The percentage differences between the observed and GLM-predicted
866 concentrations of the air pollutants during APEC and Parade.

Pollutants	Units	During APEC			During Parade		
		Observed	Predicted	Percentage differences[1]	Observed	Predicted	Percentage differences[1]
$PM_{2.5}$	μg m^{-3}	48	67	28%	15	20	25%
OC		11.2	12.6	11%	4.0	3.7	-8%
EC		1.7	2.7	37%	0.8	1.2	33%
SO_4^{2-}		3.9	2.7	-44%	2.6	5.2	50%
NO_3^-		10.6	19.0	44%	1.5	3.4	56%
NH_4^+		4.8	5.5	13%	1.5	2.4	38%
Cl^-		2.06	2.58	20%	0.16	0.17	6%
K^+		0.65	1.03	37%	0.18	0.24	25%
Pb	ng m^{-3}	55	70	21%	9	17	47%
Zn		128	171	25%	20	41	51%
Mn		34.5	51.5	33%	3.6	7.6	53%
SO_2	ppb	3.32	6.59	50%	0.57	0.56	-2%
NO_x		45	102	56%	13	20	35%
OC+EC	μg m^{-3}	12.9	15.3	16%	4.8	4.9	2%
SNA	μg m^{-3}	19.3	27.2	29%	5.6	11.0	49%
total S[2]	μmol m^{-3}	0.189	0.322	41%	0.053	0.079	33%

[1]Percentage difference = (Predicted - Observed)/Predicted × 100%.

[2]total S = $[SO_2]$ + $[SO_4^{2-}]$.

867

868

869

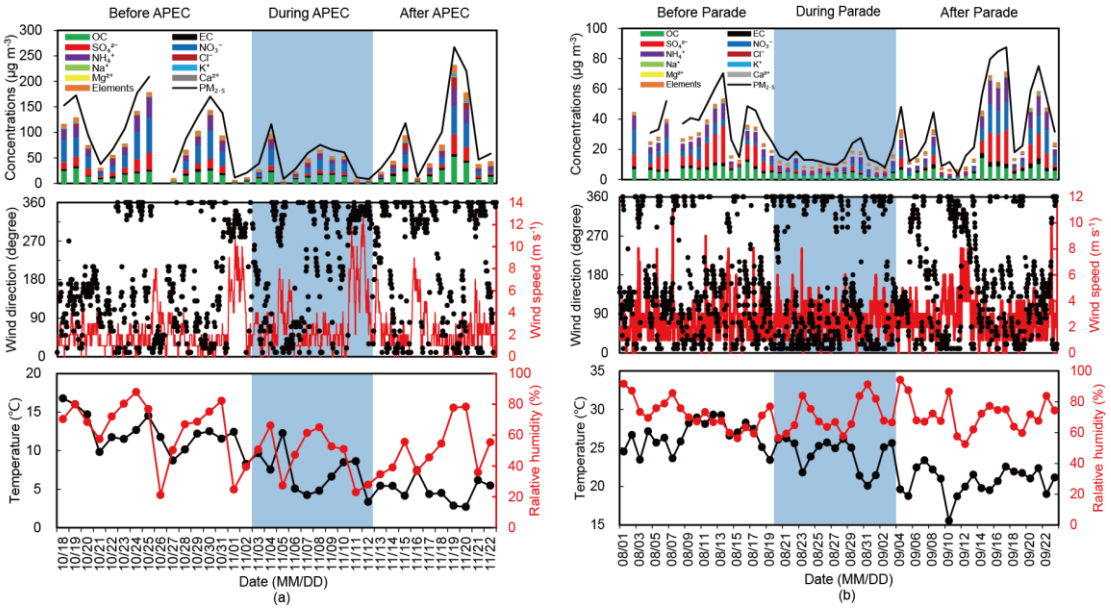

870

871 Figure 1. Time series of atmospheric particulate matter of aerodynamic diameter ≤ 2.5

872 μm ($PM_{2.5}$) and the concentrations of its components, wind direction (WD), wind speed

873 (WS), temperature (T), and relative humidity (RH) before, during, and after (a) APEC

874 2014 and (b) Parade 2015. The blue-shaded areas highlight the pollution control periods

875 of APEC 2014 (3 November to 12 November 2014) and Parade 2015 (20 August to 3

876 September 2015).

877

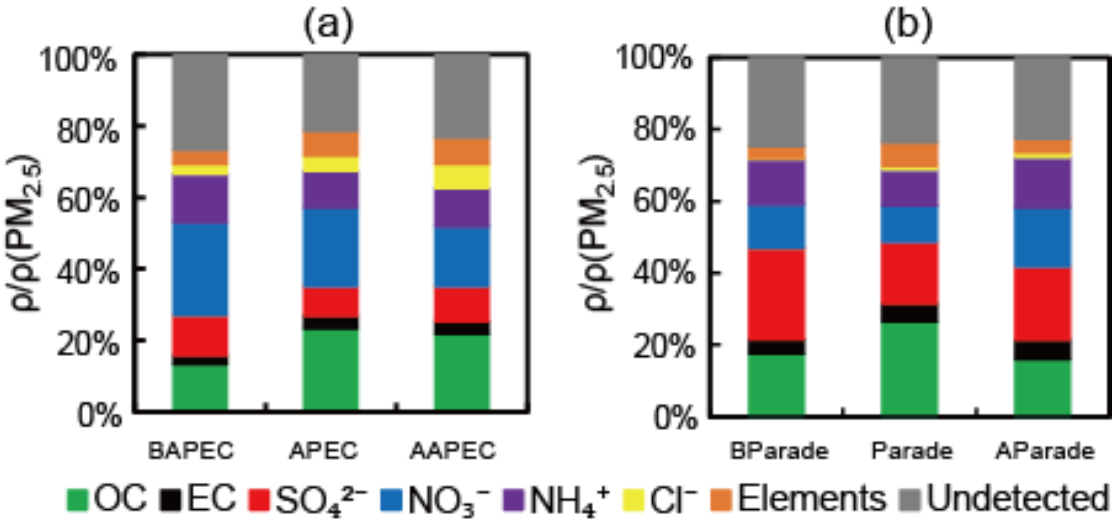

878

879 Figure 2. Proportions of the measured components in $PM_{2.5}$ during (a) APEC 2014 and

880 (b) Parade 2015 campaigns, including organic carbon (OC), elemental carbon (EC),

881 SO_4^{2-}, NO_3^-, NH_4^+, Cl^- and elements. BAPEC/BParade: before APEC/Parade,

882 AAPEC/AParade: after APEC/Parade.

883

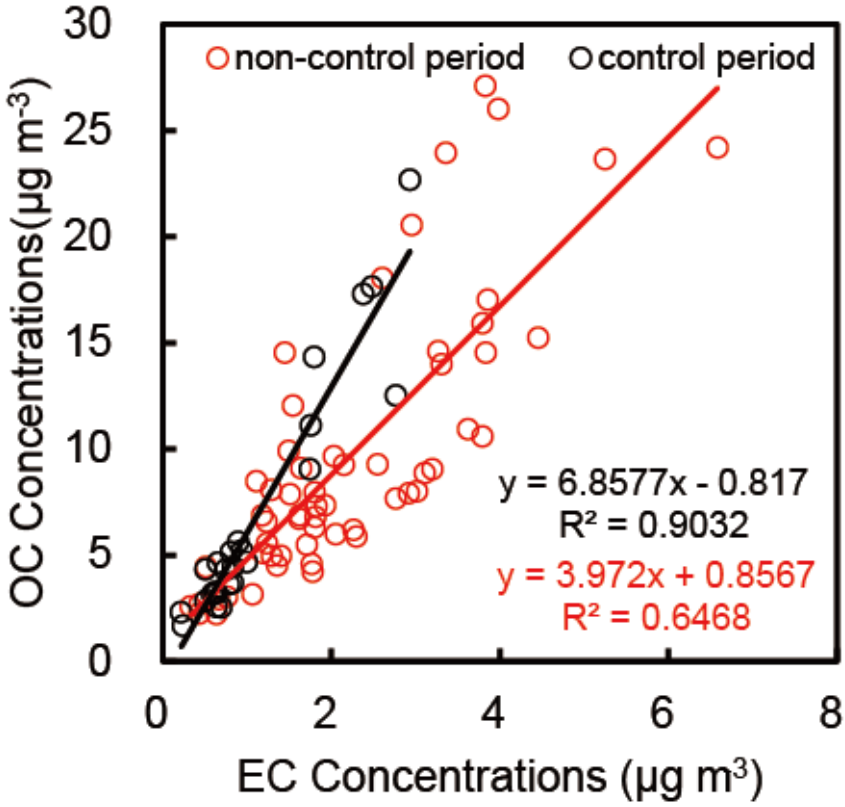

884

885 Figure 3. Scatter plot and correlations between organic carbon (OC: *y*-axis) and

886 elemental carbon (EC: *x*-axis) concentrations of $PM_{2.5}$ during the APEC 2014 and

887 Parade 2015 campaigns. The red symbols denote the non-control period and the black

888 symbols denote the pollution control period. The linear regression equations and R^2

889 values are given for these two campaigns.

890

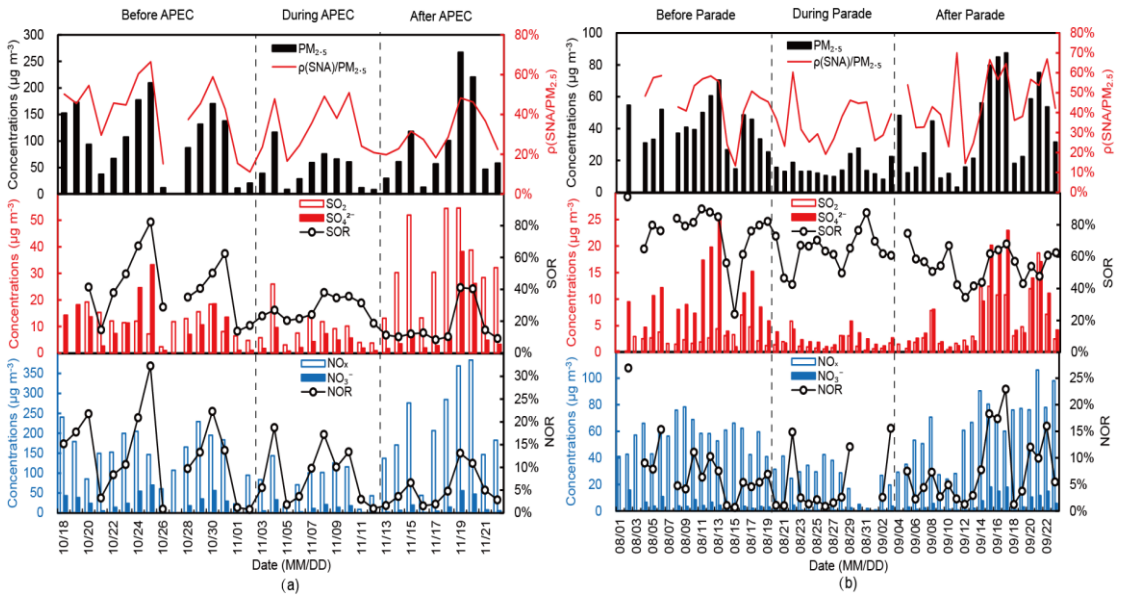

Figure 4. Upper panel: time series of the proportion of sulphate, nitrate, and ammonia (SNA) in $PM_{2.5}$ ($\rho(SNA/PM_{2.5})$) and $PM_{2.5}$ mass concentrations (the black bar represents $PM_{2.5}$ concentration and the red line represents $\rho(SNA/PM_{2.5})$). Middle panel: SO_2, SO_4^{2-}, and SOR ($[SO_4^{2-}]/([SO_2]+[SO_4^{2-}])$). Lower panel: NO_x, NO_3^-, and NOR ($[NO_3^-]/([NO_x]+[NO_3^-])$). Data collected during the (a) APEC 2014 and (b) Parade 2015 campaigns. The hollow bars represent gaseous pollutants (red for SO_2, blue for NO_x), and solid bars represent secondary inorganic ions (red for sulphate, blue for nitrate).

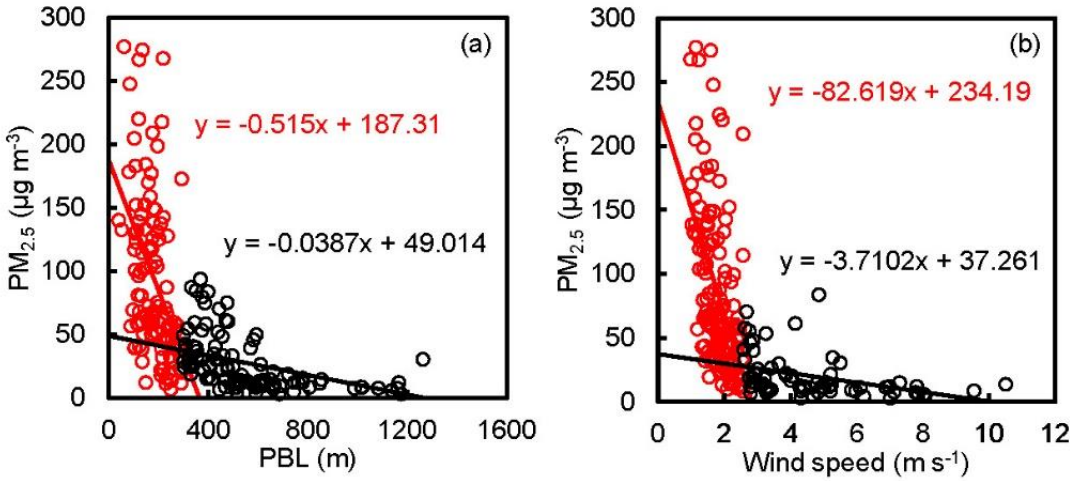

Values of intersections

PBL (m)	Wind speed (m s^{-1})
290	2.50

905

906 Figure 5. Scatter plot showing the correlation between daily $PM_{2.5}$ concentrations (*y*-
907 axis) and (a) daily PBL heights (*x*-axis) and (b) daily WSs (*x*-axis) during the sampling
908 periods. The red and black scattered points represent different distribution areas. The
909 piecewise function regression equations and the corresponding values of PBL height
910 and WS according to the intersections are given.

911

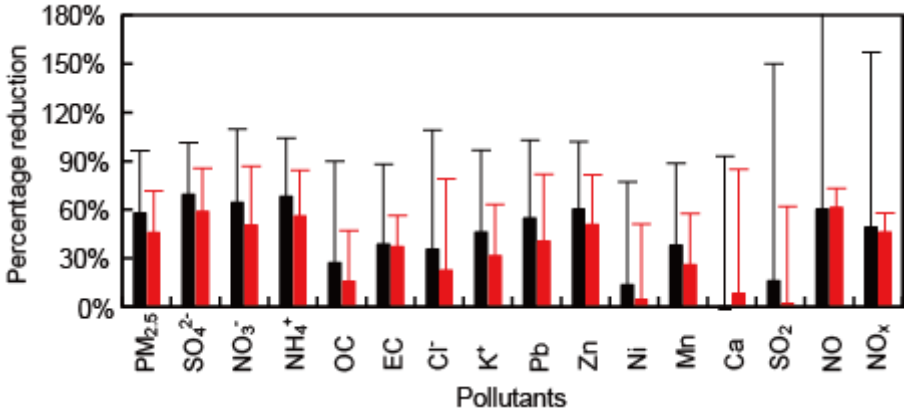

912

913 Figure 6. The percentage reductions of pollutant concentrations under similar
914 meteorological conditions. The black bars represent the percentage reductions
915 calculated by comparing the decreased average concentrations during APEC to the
916 average concentrations before APEC. The red bars represent the percentage reductions
917 calculated by comparing the decreased average concentrations during APEC to the
918 average concentrations before APEC based only on the days with stable meteorological
919 conditions. The whiskers represent the standard deviations of the percentage reductions.

920

921

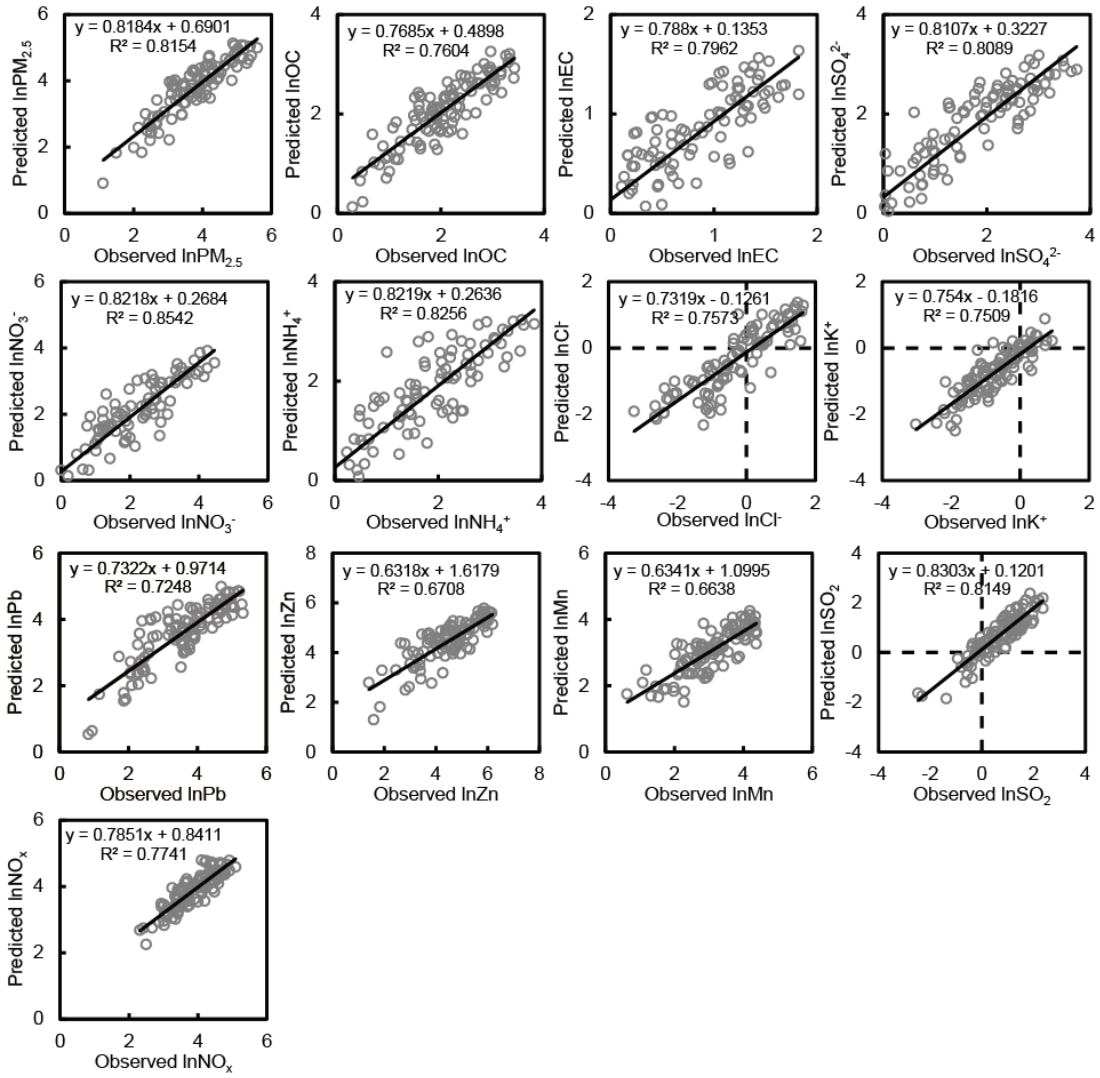

922

923 Figure 7. Scatter plot and correlations between GLM-predicted (*y*-axis) and observed

924 (*x*-axis) concentrations of pollutants transformed to a natural log. The linear regression

925 equations and R^2 values are given.

926

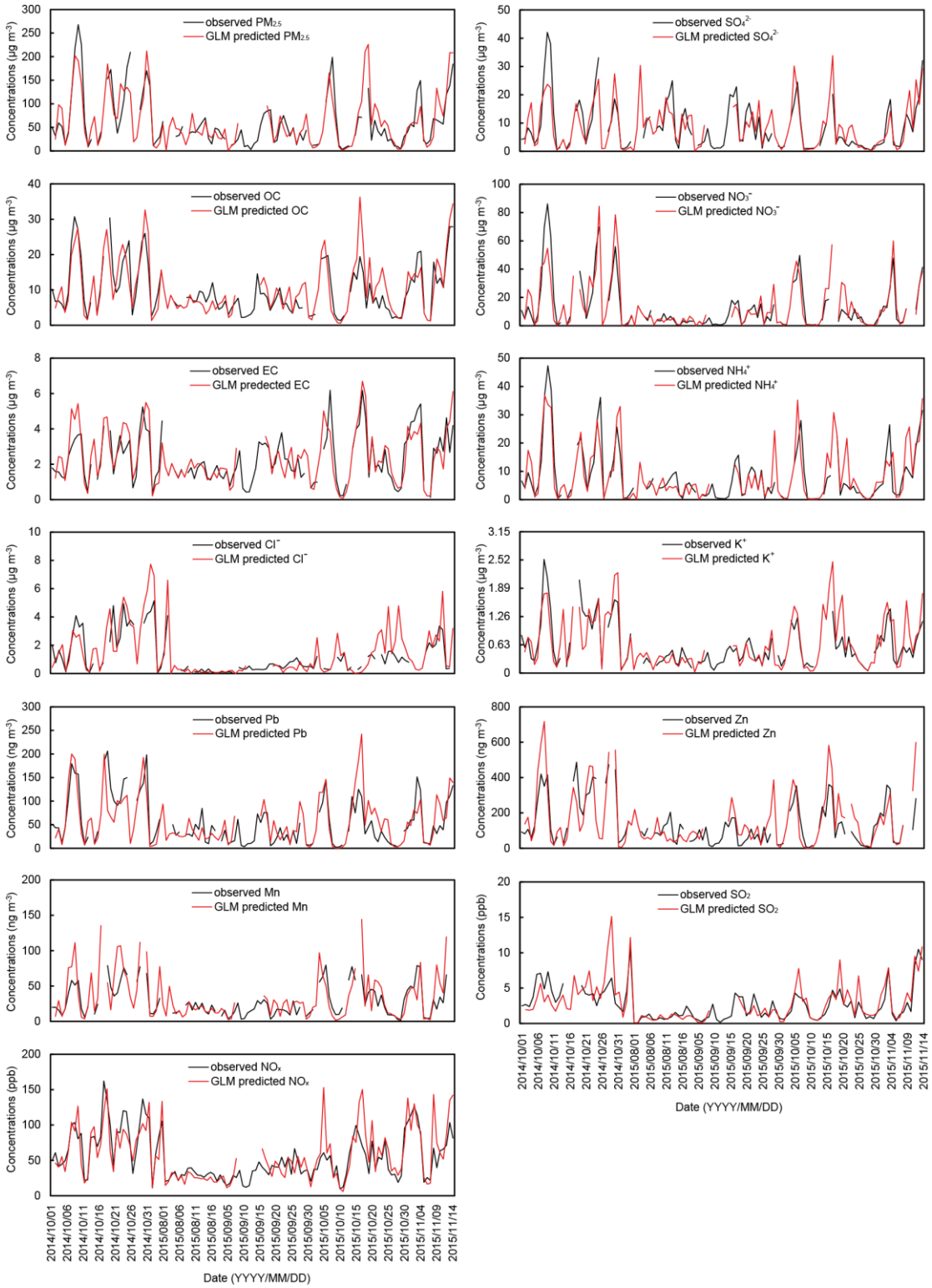

Figure 8. Time series of the observed (in black line) and GLM-predicted pollutant concentrations (in red line).

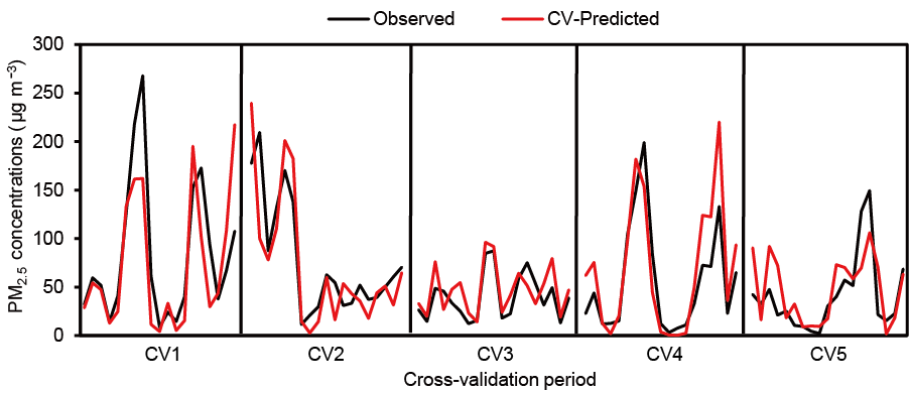

931

932 Figure 9. Time series of the observed and cross-validation (CV) predicted $PM_{2.5}$

933 concentrations during five CV periods. The black line represents the observed $PM_{2.5}$

934 concentration and the red line represents the CV-predicted $PM_{2.5}$ concentration.

935

936